Advanced finite element analysis of deep excavations using Abaqus

Yuepeng Dong[1*], Harvey J. Burd[2], Guy T. Houlsby[2], and Andrew J. Whittle[3]

1, Singapore-MIT Alliance for Research and Technology, previously University of Oxford

2, University of Oxford, UK

3, Massachusetts Institute of Technology, USA

*Corresponding author, Email: yuepeng.dong@smart.mit.edu

Abstract: Deep excavation, widely used for underground constructions, is a very complex soil-structure interaction problem in geotechnical engineering. Its performance is influenced by the sophisticated soil behavior, complex retaining structures, and variable construction sequences. As the excavation goes deeper and larger in scale, challenges arise for both practical applications and research. Finite element analysis is an effective tool to study its mechanism, which can consider both geotechnical and structural aspects. It provides necessary information on the performance of deep excavations for design purpose, and can also be used to predict the behavior of deep excavation and provide guidance for the construction. The main issues involved with the finite element analysis of deep excavations include selecting appropriate constitutive models for soils and structures, the simulation of the construction procedure, and the modelling of the soil/structure interface. These issues are addressed in detail based on the use of Abaqus. The application of this procedure is demonstrated through a detailed analysis of a deep excavation case history. Results showed that the finite element analysis can capture the performance of the deep excavation satisfactorily.

Key words: Deep excavations, finite element analysis, case histories

1 Introduction

Deep excavations are widely used in urban areas for the development of underground space, e.g. subway stations, basements for high-rise buildings, underground car parks and shopping centres. However, the excavation process inevitably alters the stress states in the ground and may cause significant wall deformations and ground movements. Especially when the excavation is close to adjacent infrastructure, e.g. buildings, tunnels, buried pipelines, piled foundations, the excavation induced ground movements must be carefully monitored and controlled within an acceptable amount, to avoid any potential damage to these classes of infrastructure.

As a very complex soil-structure interaction problem, the performance of deep excavations is influenced by the sophisticated soil behavior, complex retaining structures, and variable construction sequences. Finite element analysis is an effective tool to study its mechanism, which can consider both geotechnical and structural aspects such as soil behavior, details of structures, and construction sequences. It provides necessary information on the performance of deep excavations for design purpose, and can also be used to predict the behavior of deep excavation and provide guidance for the construction.

Advanced finite element analysis of deep excavations should adopt accurate modelling procedures for geotechnical and structural behavior, e.g. (i) the geometry of the excavation, (ii) detailed retaining structures, (iii) correct construction sequence, and (iv) reliable material models and input parameters.

The main issues involved with finite element analysis of deep excavations include selecting appropriate constitutive models for soils and structures, the simulation of the construction procedure, and the modelling of the soil/structure interface (Potts & Zdravkovic 2001). These issues are addressed in detail in this paper based on the use of Abaqus version 6.11. The application of this procedure is demonstrated through a detailed analysis of a deep excavation case history. Results showed that the finite element analysis can capture the performance of the deep excavation satisfactorily.

This paper is mainly based on relevant research conducted at University of Oxford and Massachusetts Institute of Technology (MIT).

2 Components in braced deep excavations

2.1 Modelling the soil

The soil is a critical part to deal with in the modelling procedure. This is particularly related to the partition and mesh of the model according to the excavation geometry, and the selection of element types and constitutive models.

The soil can be modelled with tetrahedral or hexahedral continuum elements in 3D analysis. For each type of elements, there are normally linear or quadratic elements (although higher order elements are also possible) with full or reduced integration. In general, quadratic elements are more accurate than linear elements in theory, but they are also expensive in calculations if the same mesh is used. Hexahedral elements are suitable for excavations with regular geometry, e.g. rectangular ones. Linear hexahedral elements with reduced integration (C3D8R) in Abaqus can be used in large scale and complex analyses, on the balance of accuracy and efficiency. However, higher order elements are recommended for more accurate purposes when computational resource is not a problem.

The performance of deep excavations is strongly influenced by the soil behavior. In finite element analysis, it is vitally important to use realistic soil models to obtain more reliable results. The selection of constitutive models largely depends on the software that is used. Abaqus includes several basic models for soils (e.g. Mohr-Coulomb, Drucker-Prager, and Modified Cam clay), and also provides the interface for advanced users to implement their specific constitutive models through the subroutine UMAT or VUMAT. A multiple-yield surface soil model (Houlsby 1999) has been implemented into Abaqus by the first author to consider the small-strain stiffness nonlinearity of the soil, and this model is used extensively at University of Oxford. Advanced soil models, MIT-E3 soil model (Whittle 1987; Whittle & Kavvadas 1994), and MIT-S1 soil model (Pestana 1994; Pestana & Whittle 1999), developed at Massachusetts Institute of Technology (MIT), have also been implemented into Abaqus and successfully used for deep excavations as well as other geotechnical problems.

2.2 The retaining wall

The retaining wall is generally modelled using either shell elements or solid elements in finite element analysis, if the wall installation process is modelled using the Wished-In-Place (WIP) method. Shell elements have no geometric thickness and are easier to generate in the mesh. In addition, the internal forces and bending moments can be obtained directly. However, it is found that the computed wall deflection and ground movement from shell element wall are larger than those from solid element wall, and this is because the shear stress on the back of soil-wall interface provides beneficial bending moment about the wall centreline when the diaphragm wall is modelled with solid elements, whereas shell element wall does not have this effect (Potts & Zdravkovic 2001; Zdravkovic et al. 2005). Moreover, when the wall installation process is modelled explicitly in the model, e.g. the Wall-Installation-Modelled method, including the trench excavation, bentonite slurry, and concrete injection, only solid elements are suitable to model the wall because the geometry of the wall needs to be considered. Therefore, solid elements are preferred to model the retaining wall in this paper. In terms of the output of internal forces and bending moments, this can be achieved through embedding the shell element wall at the centreline of solid element wall and assigning shell element wall with the same thickness of the retaining wall but a small Young's modulus if the wall is assumed as a linear elastic material. The low stiffness of the embedded shell element wall will not affect the deformation of soil element wall, but the internal forces and bending moments can be computed from the output of shell element wall.

Another issue related to the retaining wall is modelling the construction joints in the wall, as shown in Fig. 1. For example, the diaphragm wall is discontinuous in the horizontal direction along the sides of the excavation because it is constructed by sections of wall panels. Consequently, it cannot sustain any significant out-of-plane bending, and the horizontal stiffness of the wall is also much smaller than the stiffness of the solid concrete. The influence of joints can be considered by using the anisotropic wall approach (Zdravkovic et al. 2005) in which the stiffness in the direction along the joints is reduced.

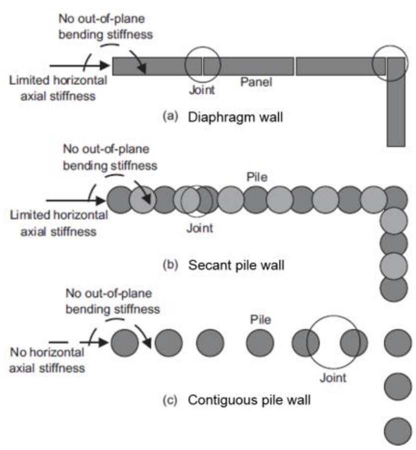

Fig. 1 Schematic view of different wall types (Zdravkovic et al. 2005)

The retaining wall is adequate to be represented by a linear elastic material for simplicity. Cracks may exist in the concrete structures and propagate during the excavation, which can be considered by reducing the nominal stiffness of the concrete components or using a more detailed concrete crack model, such as the concrete damaged plasticity model in Abaqus. However, using a more sophisticated concrete model will increase the complexity of the analysis.

2.3 The supporting system

The support system usually consists of horizontal components (e.g. reinforced concrete beams and floor slabs, and temporary steel struts), and vertical components (e.g. piles and columns). In finite element analysis, beam elements can be used to model the beams, piles, columns and steel struts, whereas shell elements are suitable for floor slabs. Opening accesses are usually designed in the floor slabs during the top-down excavation, and they can be modelled explicitly in the model.

In a similar way to the material model used for the retaining wall, the reinforced concrete components in the support system can also be assumed to behave linear elastically for simplicity or represented by a detailed concrete crack model. The concrete beams and floor slabs will shrink or expand during the curing process and due to the variation of ambient temperature, which may have large influence on the excavation behaviour. The thermal effects can be considered in the analysis by introducing thermal strains. Moreover, gaps may develop at the connection between the retaining wall and horizontal bracing structures, and concrete floor slabs may creep under service condition, which has the tendency to induce larger wall deformations. These effects can also be approximated by using the thermal shrinkage method.

2.4 Adjacent infrastructure

The adjacent infrastructure close to the excavations, e.g. buildings, utility pipelines, tunnels, and pile foundations, may be included in the model if they are major concerns in the project, although this would increase the complexity of the analysis. An example of this approach is given in Dong (2014) in which the settlements of buildings and buried pipelines are investigated.

2.5 Constraints and contacts

The connections between different structural components (e.g. retaining walls, concrete beams, floor slabs, and vertical piles) in deep excavations are usually assumed to be rigid (e.g. cast or welded) in numerical analyses, but they may be more complicated in reality (e.g. pined connections, and gaps) and they may change as the excavation proceeds. For simplicity, tie constraints are usually applied at the connections of these components in the analyses.

The interface behavior between the soil and structures (mainly the soil/wall interface and the soil/pile interface) can be modelled using contact pairs at the interface associated with a contact model. However, it should be noted that contact is a highly complex mechanism and may cause numerical difficulties. An extended Coulomb frictional contact model is available in Abaqus. Modification of this model is described later in this paper, and the influence of interface properties on the excavation behavior is investigated through parametric studies in Dong (2014).

2.6 Boundary conditions

The region to be analysed in deep excavations is of relatively small dimensions compared with those of the surrounding medium. In finite element analysis, the normal practice is to extend the mesh to some distance away from the zone of interest, and apply fixed displacement boundary conditions there.

3 Material models

3.1 Constitutive models for the soil

The built-in soil models in Abaqus are conventional and do not contain modern concepts of soil modelling, e.g. small-strain stiffness nonlinearity, recent stress history, and anisotropy. Fortunately, Abaqus provides interfaces for advanced users to implement their own constitutive models through subroutines UMAT and VUMAT. Advanced soil models are crucial to capture the sophisticated soil behavior and improve the accuracy of the analyses. Three advanced soil models are described here.

3.1.1 Multiple-yield surface soil model

A multiple-yield surface soil model (Houlsby 1999) has been implemented into Abaqus by the first author using UMAT to consider the small-strain stiffness nonlinearity of the soil. This soil model takes into account the non-linear behavior of soil at small strains, and also includes effects such as hysteresis and dependence of stiffness on recent stress history. It uses multiple yield surfaces within the framework of work-hardening plasticity theory. Non-linearity of the small-strain response is achieved using a number of nested yield surfaces of the same shape as the outer fixed failure surface. Those inner yield surfaces translate as the stress state changes, while the bounding von Mises failure surface models perfect plastic behavior with no work hardening. As a stress point moves in the stress space and encounters a yield surface as shown in Fig.2, the stiffness reduces as shown in Fig.3, and the yield surface moves with the stress point. It thus models the non-linearity of response at small strains, and the effect of recent stress history.

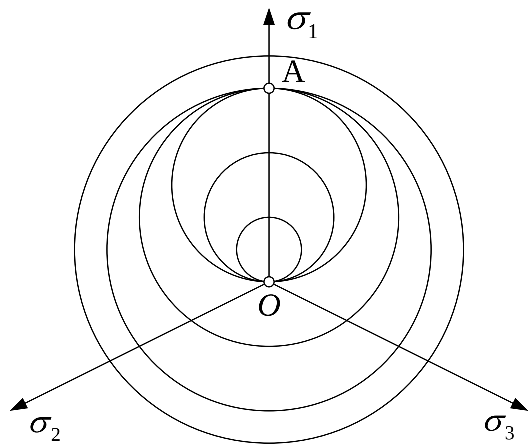

Fig.2 Yield surface after stress path from O to A and back to O (Houlsby 1999)

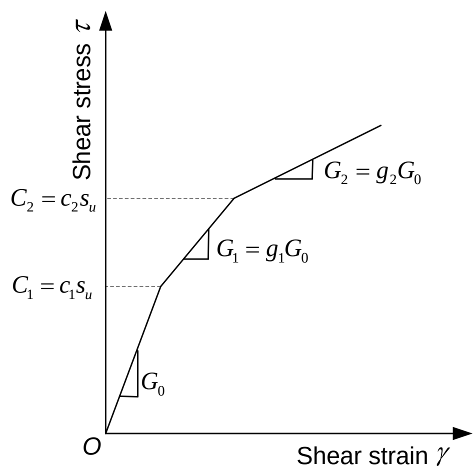

Fig.3 Shear stress-strain cure

The model is specified by the small strain shear modulus, G_0, the bulk modulus K and a set of non-dimensional parameters c_i and g_i ($i = 1, n$) that are used to specify the size and work hardening characteristics of each of the inner surfaces. The size of each inner surface is $c_i C$ and the tangent shear modulus when the i^{th} surface is active is $g_i G_0$. A total of nine inner yield surfaces are used in the analyses described in this paper, a balance between accuracy and computational efficiency. Calibration of this soil model for Shanghai Clay is described in Dong (2014). This soil model has been applied to tunneling (Burd et al. 2000) and deep excavations (Dong 2014) with success.

3.1.2 MIT-E3 soil model

The MIT-E3 soil model (Whittle 1987; Whittle & Kavvadas 1994) is an advanced constitutive model which captures the nonlinear and inelastic behavior of normally consolidated to lightly consolidated clay (OCR<8) such as (i) small-strain stiffness nonlinearity, (ii) anisotropic stress-strain-strength, and (iii) hysteretic and inelastic behavior due to cyclic loading. The model is formulated based on the theory of incrementally linearized elasto-plasticity and consists of three distinct components: (i) an elasto-plastic model for normally consolidated clays, (ii) a perfectly hysteretic formulation, and (iii) bounding surface plasticity. Fig. 4 shows the shape of the yield, failure and loading surfaces used in the MIT-E3 model.

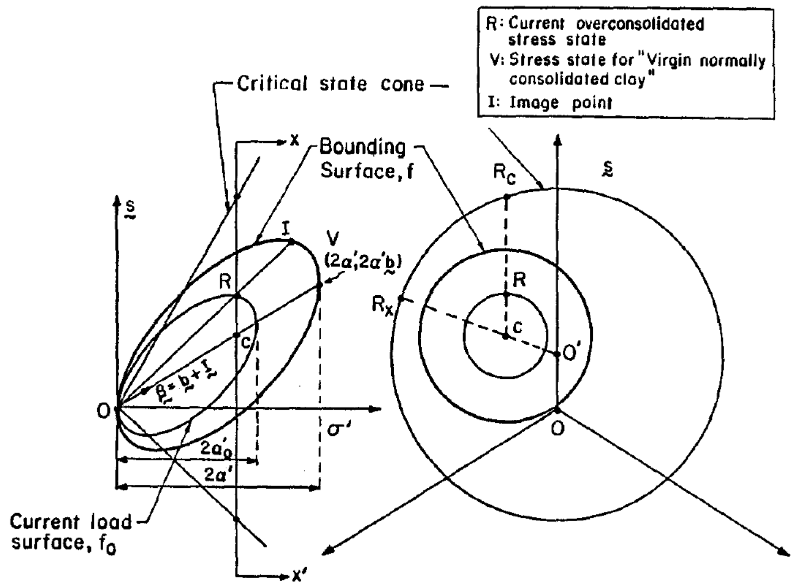

Fig. 4 Yield, failure and load surface of MIT-E3 soil model (Whittle & Kavvadas 1994)

The model has 15 material constants and a series of state variables describing (i) the effective stresses, (ii) the size and orientation of the bounding surface, (iii) the effective stresses at the most recent reversal state, (iv) the strain accumulated since the last reversal state, (v) the size of the bounding surface at the last reversal state, and (vi) the size of the load surface at first yield. This soil model has been implemented to Abaqus by Hashash (1992), and extensively used in deep excavations (Whittle et al. 1993; Hashash & Whittle 1996) as well as other geotechnical analyses.

3.1.3 MIT-S1 soil model

MIT-S1 model (Pestana 1994; Pestana & Whittle 1999) is a generalized effective stress soil model, for describing the rate independent behavior of freshly deposited and over-consolidated soils. It is a third generation of soil model, developed at MIT, after MIT-E1, and MIT-E3. It inherits the basic structure of its predecessors (MIT-E3), but also introduces significant improvements in the form of the bounding surface and hardening laws. A new framework of compression behavior unifies the modelling of clays and sands. The model introduces new expressions for describing small-strain non-linearity, therefore enhancing predictions of shear modulus degradation for both clays and sands. The model also incorporates a variable Poisson's ratio to describe more realistically the variation of K_0 measured during one-dimensional swelling and subsequently reloading. Fig. 5 shows the bounding surface of MIT-S1 soil model and compares with isotropic yield surface of Modified Cam Clay model and anisotropic bounding surface of MIT-E3 model.

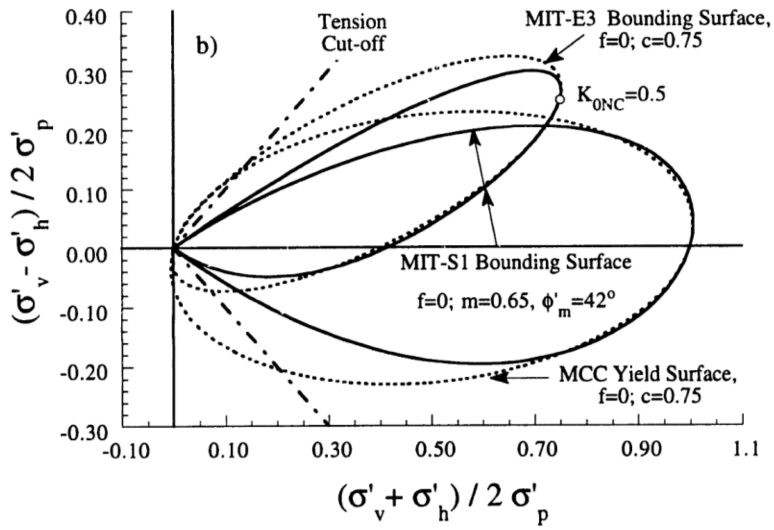

Fig. 5 Comparison of yield surfaces of MIT-S1 with MCC and MIT-E3 (Pestana & Whittle 1999)

The model requires, in general, 16 input parameters to characterize a general soil specimen. Typical predictions for sands or clays, on the other hand, requires only 14 or 13 parameters, respectively. Evaluation of this soil model on sands and clays are shown in (Pestana, Whittle & Salvati 2002) and (Pestana, Whittle & Gens 2002) respectively. The MIT-S1 soil model has also been implemented to Abaqus, and application of this model to deep excavations in Berlin Sands can be referred to Nikolinakou et al. (2011).

3.2 Constitutive models for the structure

The structural components in deep excavations (e.g. the diaphragm wall, horizontal beams and floor slabs, and vertical piles) are mainly reinforced concrete structures, and it is adequate to model them as a linear elastic material for simplicity. The effect of cracks is normally considered by reducing the nominal value of the Young's modulus of the intact concrete.

Abaqus provides several more realistic models for reinforced concrete structures, e.g. the concrete smeared cracking model, and concrete damaged plasticity model, for advanced analyses. The concrete damaged plasticity model in Abaqus provides a general capability for modelling reinforced concrete structures. It uses concepts of isotropic damaged elasticity in combination with isotropic tensile and compressive plasticity to represent the inelastic behavior of concrete. It consists of the combination of non-associated multi-hardening plasticity and scalar (isotropic) damaged elasticity to describe the irreversible damage that occurs during the fracturing process. However, the disadvantage of using these models is associated with the difficulties in determining the large number of material parameters and the numerical instabilities during the calculation.

As discussed earlier in this paper, the retaining wall is discontinuous in the horizontal direction and has construction joints in the wall. The anisotropic wall approach (Zdravkovic et al. 2005) is an adequate method to consider the effect of construction joints. The retaining wall is modelled as a cross anisotropic linear elastic material to investigate its capability in capturing the observed excavation behavior (Dong 2014). For the local coordinate system in Fig.6, the Young's modulus E along 2-direction is reduced by a factor of $\beta(\beta < 1.0)$, while the material is isotropic in 1-3 plane.

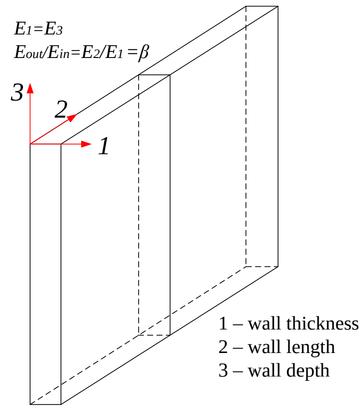

Fig.6 Local directions for cross anisotropic wall

Thermal effects of concrete beams and floor slabs, as discussed earlier in this paper, may affect the wall deformation and ground movement. This can be considered in the concrete material properties by specifying a coefficient of thermal expansion α , and a temperature change ΔT .

3.3 Constitutive models for the soil/structure interface

An extended version of the classical isotropic Coulomb friction model is available in Abaqus for use with general contact analysis capabilities. The extensions include an additional limit on the allowable shear stress, anisotropy and the definition of a secant friction coefficient. The standard Coulomb friction model assumes that no relative motion occurs if the equivalent frictional stress $\tau_{eq} = \sqrt{\tau_1^2 + \tau_2^2}$ (where τ_1 and τ_2 are shear stresses on the interface), is less than the critical stress τ_{crit} which is proportional to the contact pressure p in the form $\tau_{crit} = \mu p$ (where μ is the friction coefficient). It is possible to put a limit on the critical shear stress, $\tau_{crit} = \min(\mu p, \tau_{\max})$, where $\tau_{\max}$ is a user specified constant. If the equivalent stress reaches the critical stress ($\tau_{eq} = \tau_{crit}$), slip will occur.

In geotechnical engineering, it is reasonable to link τ_{crit} with the undrained shear strength of the soil s_u , e.g., $\tau_{crit} = \alpha \cdot s_u$, where α is an coefficient. Further modification can be made through a subroutine FRIC to make $\tau_{\max}$ as a variable. This modified version of the extended Coulomb friction model is illustrated in Fig.7. The influence of the value of α on the excavation behaviour is investigated through a number of parametric studies in Dong (2014).

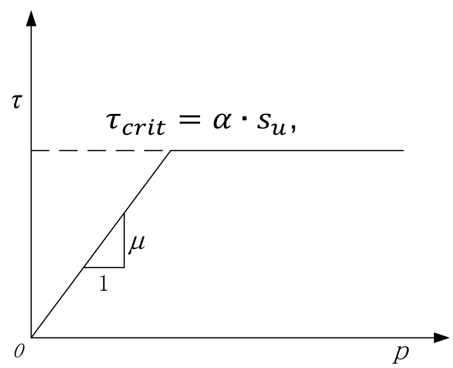

Fig.7 Extended Coulomb friction model

4 Modelling procedures

4.1 Geostatic analysis

Geostatic stress-displacement analysis is the first step for equilibrium iteration to set up the initial stress state in the ground prior to the construction. The vertical stress is governed by the gravity, while the horizontal stresses are related to the vertical stress through the coefficient of lateral earth pressure at rest K_0. There are well established procedures to define the value of K_0 in both normally consolidated and overly consolidated soil.

4.2 Wall and pile installation

The diaphragm wall is a cast-in-situ reinforced concrete retaining wall constructed using a slurry supported trench method. The installation process includes deep mixing, slurry supported excavation, placing the reinforced cage, concrete casting and curing. The bored pile installation follows the similar process. The installation process modifies the in-situ stress state in the ground close to the trench and influences the starting point for analysis of the post-construction behaviour. In addition, it results in substantial ground movements and settlements of adjacent infrastructure, which may be significant compared to those induced by the excavation itself. The influence depends on the groundwater level, panel width, and changes in pore water pressure during diaphragm wall installation. Therefore, although simple, the widely used Wished-In-Place (WIP) method for the wall and pile installation in the finite element analyses of deep excavations neglects the installation effect on the ground movement and the subsequent excavation behaviour.

The effects of diaphragm wall installation have been investigated through finite element analyses by several researchers, e.g. Ng & Lings (1995), Ng & Yan (1999), Gourvenec & Powrie (1999), and Burlon et al. (2013). The construction of a single panel is modelled by the following procedure:

1) Excavate the trench and apply the hydrostatic bentonite pressure on the trench surfaces simultaneously;
2) Cast the panel with concrete by increasing the lateral pressure inside the trench to a bilinear wet concrete pressure envelope as proposed by Lings et al. (1994);
3) Cure the concrete panel by replacing the trench with concrete material and remove the applied bilinear concrete pressures simultaneously.

4.3 Soil removal and structure installation

The soil excavation and structure installation can be modelled by deactivating or reactivating the corresponding finite elements in the model. When the elements are deactivated in the analysis, the contribution of mass and stiffness of that element is removed from the global Mass and Stiffness matrix.

4.4 Dewatering and consolidation

A dewatering process is normally used inside the excavation when the ground water table is high, e.g. in Shanghai. The dewatering and consolidation processes can be conducted using a displacement-pore pressure coupled analysis with an effective stress soil model. The general process in the finite element analysis is described in this section, although they are not modelled in the analyses in this paper, due to the limitation of the soil model used. The pore water pressure at the ground water table level and the excavated soil surface is set to zero in the analysis. Changes of pore water pressure with time are calculated with the drainage boundary conditions and specification of permeability and consolidation characteristics of the soil. Detailed analysis can be seen in Zheng et al. (2014)

5 Analysis of deep excavation case histories

Application of the previous procedures will be demonstrated through a detailed study of a well-documented deep excavation case history.

5.1 General description of the case history

Shanghai Xingye Bank building is a high-rise building (82.5m high) with a three-level basement. The structure is constructed from a reinforced concrete frame and the building is founded on deep piles (Xu 2007). Construction of the basement began in February 2002, and finished in December 2003. The excavation depth, as shown in Fig. 8, is 14.2m on the west side, and 12.2m on the east side. The excavation is surrounded by a number of densely packed buildings and several old service pipes. Ground improvement (e.g. root piles, and spiral injection piles), therefore, was conducted outside the excavation to mitigate the detrimental effects on the buildings. A comprehensive field measurement was conducted during the excavation process. This site is situated on typical Shanghai Clay which is composed of Quaternary sediments and has high water content, low shear strength, and high compressibility.

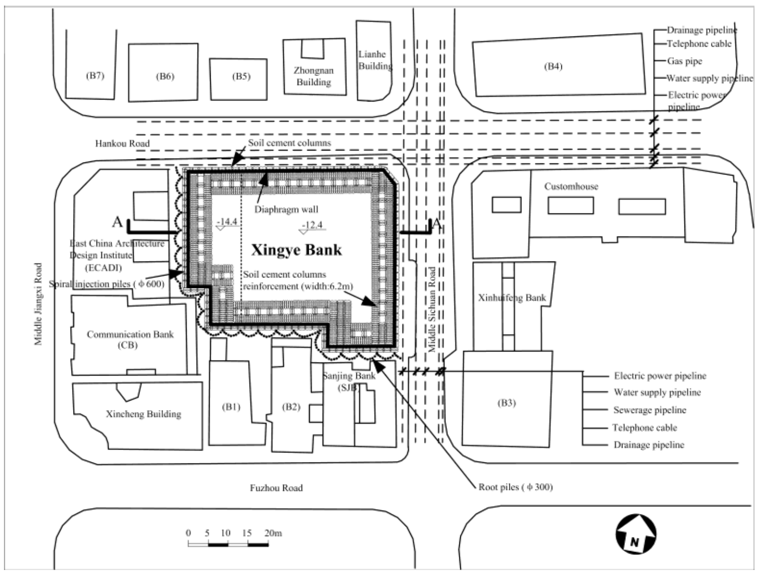

Fig. 8 Plane view of adjacent infrastructure (Xu 2007)

The A-A sectional view of the excavation in Fig. 9 shows briefly the structure of the retaining system which is mainly composed of the diaphragm wall, horizontal beams and floor slabs, and vertical piles and columns.

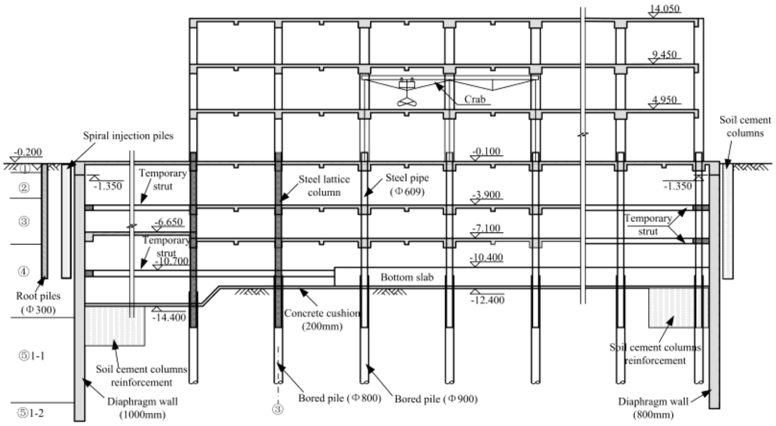

Fig. 9 Layout of instrumentation at the construction site (Xu 2007)

5.2 Finite element model

A detailed 3D finite element model was created to represent at an appropriate level of detail of structure and various construction sequences.

The soil and diaphragm wall are modelled with 8-noded solid hexahedral elements with reduced integration (C3D8R). The support system includes vertical piles, horizontal beams, and floor slabs. The piles and beams are modelled with 3D 2-noded beam elements (B31), while the floor slabs are modelled with 4-noded quadrilateral shell elements with reduced integration (S4R). Three adjacent buildings (i.e., ECADI building, CB building, and SJB building, as shown in Fig. 8) are included in the model. The external and internal walls, as well as the floor slabs, are modelled with linear quadrilateral shell elements with reduced integration (S4R). The bottom of the building is embedded into the piled-raft foundation which is modelled with solid and beam elements. The ground improvement around the excavation, as shown in Fig. 8, is represented by shell elements for simplicity. Two buried pipelines (see Fig. 8) on two sides of the exuviation are modeled using beam elements.

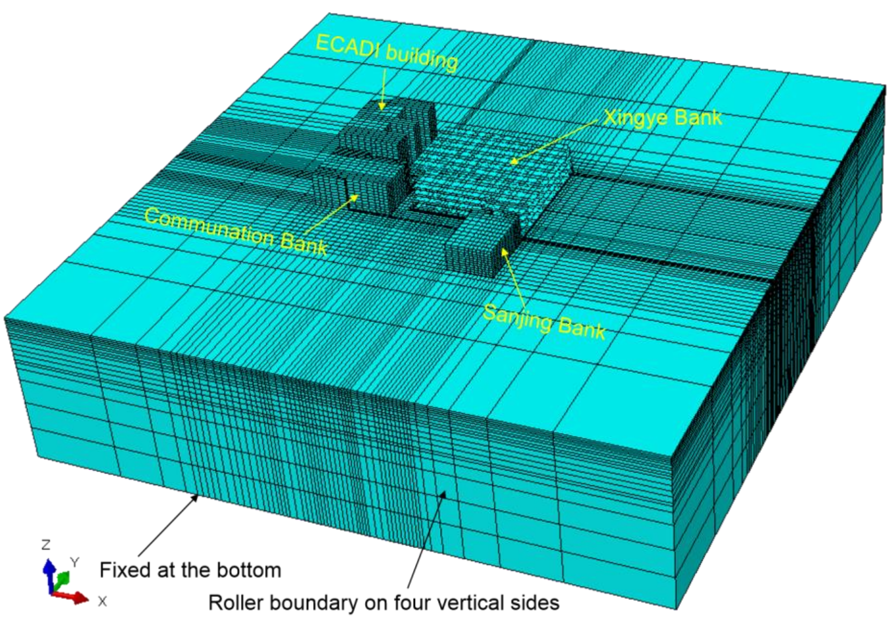

Fig. 10 Mesh and boundary conditions of the model

The soil is represented by the multiple surface plasticity model, as described earlier in the paper. The stiffness G_0 and shear strength s_u parameters increase linearly with depth. The diaphragm wall and the surrounding ground improvement are modelled as a anisotropic linear elastic material to consider the joints in the wall. The horizontal beams and floor slabs are modelled as a linear elastic material with thermal effects. The buildings are assumed to behave linear elastically because no obvious cracks or damage were observed in the buildings during and after the excavation. The piles and pipelines are also assumed to be a linear elastic material.

The analysis is conducted in undrained conditions considering the short period of construction and low permeability of the clay. The real construction sequence is followed in the analysis.

5.3 Computed results

Correlation between the numerical results and field measurement, presented in Dong (2014), indicates that the advanced finite element analysis can reproduce the observed excavation behaviour satisfactorily. This section only shows some displacement contours of ground and structures at the final stage of the excavation.

The vertical displacement of the whole model is shown in Fig. 11. As can be seen, the soil inside the excavation moves upwards due to the stress relief caused by the soil removal, while the soil outside the excavation settles down, and the settlement is larger behind the wall centre but smaller around the wall corner, indicating the 3D effect or corner effect. The adjacent buildings settle with the ground, and the settlement is larger close to the diaphragm wall and becomes smaller far away from the excavation, which means the building inclines towards the excavation. It also shows that the ECADI building settles more than the other two buildings.

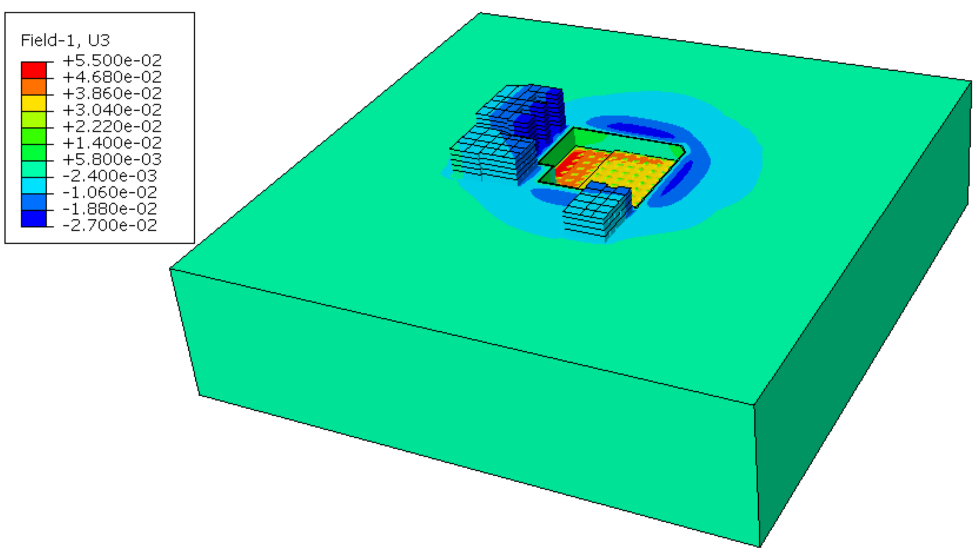

Fig. 11 Vertical displacement of whole model (unit:m)

As shown in Fig. 12, the largest wall deflection is concentrated at the wall centre area close to the excavation formation level, while the deflection at the corner is smaller due to the corner effect. The shape of the diaphragm wall also affects the wall deflection. For example, the wall deflection is larger in the longer piece of wall, while smaller in the shorter piece of wall.

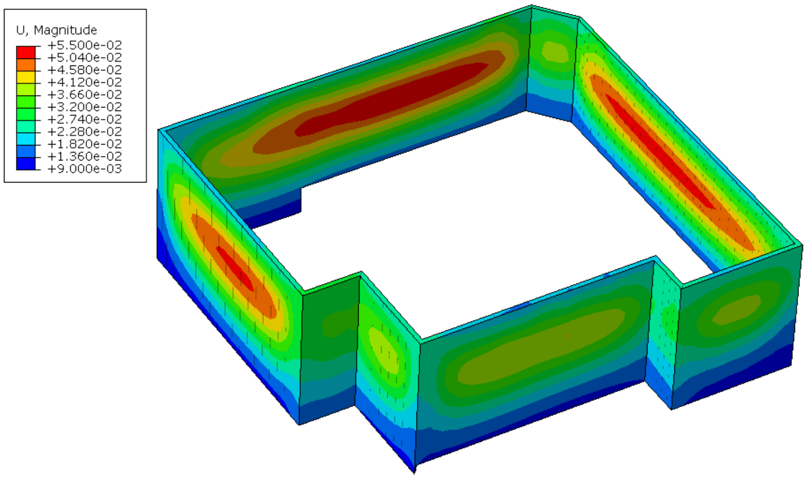

Fig. 12 Wall deflection (unit:m)

The displacement contour of the support system is shown Fig. 13. The piles move upwards due to basal heave. The displacement of beams and slabs are constrained by diaphragm wall and piles, and the differential settlement is clearly seen which may cause cracks inside the concrete.

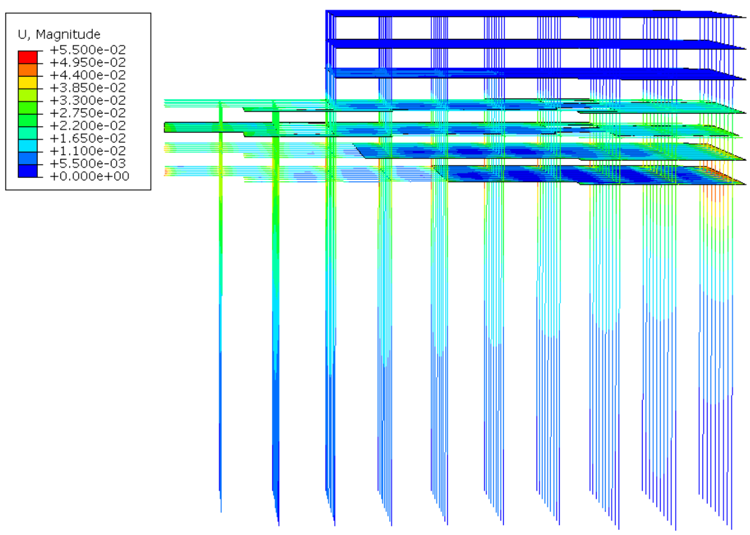

Fig. 13 Displacement distribution of the supporting system

As shown in Fig. 14, the ground improvement deforms with the ground and the pattern is similar to the diaphragm wall deformation. The deformation is larger behind the centre of the diaphragm wall at the final excavation formation level, and smaller at the corner.

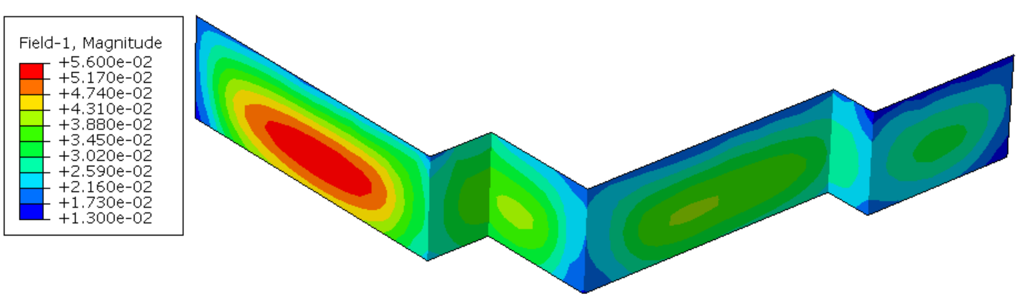

Fig. 14 Deformation of the ground improvement (unit:m)

It can be seen in Fig. 15 that the settlement of the buried pipelines is mainly concentrated in the region behind the excavation, which confirms that the excavation has a large impact on the adjacent buried pipelines.

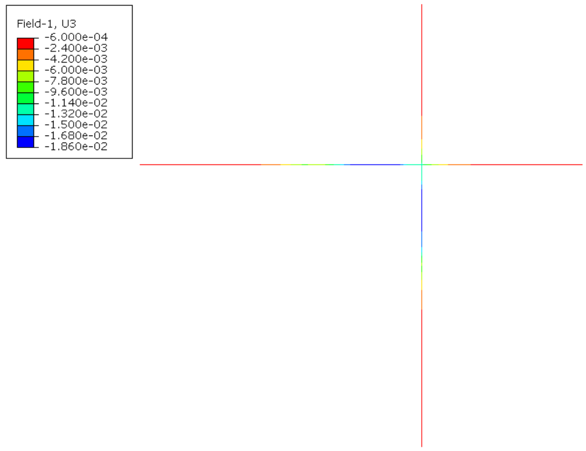

Fig. 15 Settlement of the buried pipeline (unit:m)

6 Conclusions

This paper discussed the procedures in advanced finite element analysis of deep excavations based on the use of Abaqus. The key components in the analysis include the soil, the retaining wall, the support system, adjacent infrastructure, constrains and contacts, and the boundary conditions. The material constitutive models are critical to capture the main excavation behaviour. The models for the soil, structures, and contact are described in details. Advanced soil models are implemented into Abaqus through UMAT, which considers more sophisticated soil behaviors such as small-strain stiffness nonlinearity, and anisotropy. An anisotropic wall approach is adopted to consider the construction joints in the retaining wall, and thermal effects are considered in the horizontal beams and floor slabs. The extended Coulomb friction model in Abaqus is modified through a subroutine FRIC, in which the shear resistance at the soil-structure interface is related to the undrained shear strength of the soil. The main modelling procedures in the analysis are also described in this paper, including the geostatic analysis, wall and pile installation, soil removal and structure installation, dewatering, and consolidation. The proposed procedure is demonstrated through a detailed study of a deep excavation case history. Results showed that the advanced finite element analysis can reproduce the observed excavation behaviour satisfactorily.

7 Acknowledgement

The main work described in this paper is based on the research conducted at University of Oxford during the DPhil study of the first author supervised by Prof Harvey J. Burd and Prof Guy T. Houlsby. The case history is kindly provided by Dr Zhonghua Xu who collected and analysed the field measurement in his PhD thesis. Extension of this work is currently undergoing with Prof Andrew J. Whittle at MIT, based in Singapore-MIT Alliance for Research and Technology.

8 References

Burd, H.J. et al., 2000. Modelling tunnelling-induced settlement of masonry buildings. *Proceedings of the Institution of Civil Engineers: Geotechnical Engineering*, 143(1), pp.17–29.

Burlon, S., Mroueh, H. & Shahrour, I., 2013. Influence of diaphragm wall installation on the numerical analysis of deep excavation. *International Journal for Numerical and Analytical Methods in Geomechanics*, 37(11), pp.1670–1684.

Dong, Y., 2014. *Advanced Finite Element Analysis of Deep Excavation Case Histories*. DPhil thesis, University of Oxford, Oxford, UK.

Gourvenec, S.M. & Powrie, W., 1999. Three-dimensional finite-element analysis of diaphragm wall installation. *Geotechnique*, 49(6), pp.801–823.

Hashash, Y.M.A., 1992. *Analysis of deep excavations in clay*. Sc.D thesis, Massachusetts Institute of Technology, Cambridge, Boston, U.S.

Hashash, Y.M.A. & Whittle, A.J., 1996. Ground movement prediction for deep excavations in soft clay. *Journal of Geotechnical and Geoenvironmental Engineering*, 122(6), pp.474–486.

Lings, M.L., Ng, C.W.W. & Nash, D.F.T., 1994. The lateral pressure of wet concrete in diaphragm wall panels cast under bentonite. *Proceedings - ICE: Geotechnical Engineering*, 107(3), pp.163–172.

Ng, C.W.W. & Lings, M.L., 1995. Effects of Modeling Soil Nonlinearity and Wall Installation on Back-Analysis of Deep Excavation in Stiff Clay. *Journal of Geotechnical Engineering*, 121(10), pp.687–695.

Ng, C.W.W. & Yan, R.W.M., 1999. Three-dimensional modelling of a diaphragm wall construction sequence. *Geotechnique*, 49(6), pp.825–834.

Nikolinakou, M.A. et al., 2011. Prediction and interpretation of the performance of a deep excavation in berlin sand. *Journal of Geotechnical and Geoenvironmental Engineering*, 137(11), pp.1047–1061.

Pestana, J.M., 1994. *A unified constitutive model for clays and sands*. ScD thesis, Massachusetts Institute of Technology, Cambridge, Boston, U.S.

Pestana, J.M. & Whittle, A.J., 1999. Formulation of a unified constitutive model for clays and sands. *International Journal for Numerical and Analytical Methods in Geomechanics*, 23(12), pp.1215–1243.

Pestana, J.M., Whittle, A.J. & Gens, A., 2002. Evaluation of a constitutive model for clays and sands: Part II – clay behaviour. *International Journal for Numerical and Analytical Methods in Geomechanics*, 26(11), pp.1123–1146.

Pestana, J.M., Whittle, A.J. & Salvati, L.A., 2002. Evaluation of a constitutive model for clays and sands: Part I - sand behaviour. *International Journal for Numerical and Analytical Methods in Geomechanics*, 26(11), pp.1097–1121.

Potts, D. & Zdravkovic, L., 2001. *Finite Element Analysis in Geotechnical Engineering: Vol. 2 - Application*, London: Thomas Telford Limited.

Whittle, A.J., 1987. *A constitutive model for overconsolidated clays with application to cyclic loading of friction piles*. ScD Thesis, Massachusetts Institute of Technology, Cambridge, Boston, U.S.

Whittle, A.J., Hashash, Y.M.A. & Whitman, R. V, 1993. Analysis of deep excavation in Boston. *Journal of Geotechnical Engineering - ASCE*, 119(1), pp.69–90.

Whittle, A.J. & Kavvadas, M.J., 1994. Formulation of MIT-E3 constitutive model for overconsolidated clays. *Journal of Geotechnical Engineering - ASCE*, 120(1), pp.173–198.

Xu, Z.H., 2007. *Deformation Behaviour of Deep Excavations supported by Permanent Structure in Shanghai Soft Deposit*. PhD thesis, Shanghai Jiao Tong University, Shanghai, China.

Zdravkovic, L., Potts, D.M. & St. John, H.D., 2005. Modelling of a 3D excavation in finite element analysis. *Geotechnique*, 55(7), pp.497–513.

Zheng, G. et al., 2014. Test and numerical research on wall deflections induced by pre-excavation dewatering. *Computers and Geotechnics*, 62, pp.244–256.